

# Identification of the mass transfer mechanisms involved in the transport of human immunoglobulin-G in *N,N,N',N'*-ethylenediaminetetramethylenephosphonic acid-modified zirconia

Sabyasachi Sarkar<sup>a</sup>, Peter W. Carr<sup>b</sup>, Anu Subramanian<sup>a,\*</sup>

<sup>a</sup> 207 Othmer Hall, Chemical Engineering, University of Nebraska, Lincoln, NE 68588-0463, USA

<sup>b</sup> University of Minnesota, Department of Chemistry, Smith and Kolthoff Halls, 207 Pleasant St. SE, Minneapolis, MN 55455, USA

Received 18 February 2004; accepted 15 April 2005

## Abstract

Zirconia particles modified with *N,N,N',N'*-ethylenediaminetetramethylenephosphonic acid (EDTPA), further referred to as r\_PEZ, were studied as a support material for use in chromatography. Our previous studies have demonstrated the utility of r\_PEZ in the separation of immunoglobulins from biological fluids. In the present study we sought to understand the underlying factors and identify the rate-limiting mechanisms that govern the transport of biomolecules in r\_PEZ. Pulse injection techniques were used to elucidate the individual mass transfer parameters. Elution profiles obtained under retained and unretained conditions were approximated by the Gaussian equation and the corresponding HETP contributions were estimated. The dependence of the HETP values on incremental salt concentration in the mobile phase was determined. Resulting data in conjunction with the equations outlined in literature were used to estimate the theoretical number of transfer units for the chromatographic separation process. Our results indicate that surface diffusion probably plays a minor role; however pore diffusion was established to be the rate limiting mechanism for immunoglobulin G adsorption to r\_PEZ. The HETP based methodology may be used to estimate the rate limiting mechanisms of mass transfer for any given chromatographic system under appropriate conditions. © 2005 Elsevier B.V. All rights reserved.

**Keywords:** Zirconia; Pseudo-affinity matrix; Immunoglobulin; Pulse-injection; HETP

## 1. Introduction

Chromatography based separation processes have gained increased importance in the downstream operations of biotechnology and pharmaceutical industries [1,2]. Scale-up and automation of chromatographic steps necessitate an understanding of the underlying mechanisms that control transport of solutes in chromatographic matrices. Development of new and improved chromatographic techniques, instruments, software and supports [3–6] are all efforts directed towards this goal.

A major factor influencing the effectiveness and efficiency of chromatographic based separations are the properties of their support matrices. Optimal design of supports for use in process-scale chromatography requires a balance among separation factors, such as binding capacity, operational flow rates and operational times [5]. Adsorption and desorption of proteins on conventional beaded supports are described as a combination of surface and pore diffusion with simultaneous adsorption or desorption; the exact mechanisms differing for different systems. Thus, the prediction and estimation of the underlying parameters that govern the transport of biomolecules in chromatographic supports is necessary for a valid scale-up and design strategy.

Identification of an appropriate isotherm model that describes the adsorption process and a relevant solute

\* Corresponding author. Tel.: +1 402 472 3463; fax: +1 402 472 6989.  
E-mail address: [asubramanian2@unl.edu](mailto:asubramanian2@unl.edu) (A. Subramanian).

transport model is an essential first step in the design methodology. Knowledge of the adsorption process may then be used to describe the separations process mathematically. Chromatographic separations are a special case of fixed-bed separations. Previous research has analyzed in detail the general theory and mechanism that govern the mass transport of solutes in chromatography [7–14]. Numerous studies have been performed that make favorable approximations to the transport equations to obtain design equations amenable to an analytical or numerical analysis—in most cases with suitable assumptions made to the rate of adsorption or to the rate limiting processes [9–12,14–17]. The assumptions were valid for the system and its operating conditions, which also could be inferred from the experimentally obtained breakthrough profiles. However, in addition to this, a prior knowledge of rate constants and rate limiting processes is often necessary. To make valid assumptions though, a prior knowledge of dimensionless parameters defining the relationship between processes, such as film mass transfer to pore diffusion is often necessary.

One way to obtain such information may be done by using pulse injection techniques [13]; where elution profiles of molecules of interest that have been ‘pulsed’ into the system, are gleaned for information that probe into the nature of the matrix. Pulse injection techniques in conjunction with classical height equivalent of a theoretical plate (HETP) equations have been used earlier to determine the transport parameters in commercially available matrices [18,21–24]. In this study we have used pulse injection techniques to characterize a zirconia based chromatographic support.

Supports based on zirconia have the potential to offer novel methodologies with novel selectivities. They also overcome the shortcomings of existing supports that are relevant for use in the preparative scale purifications [19]. We have reported the preparation of zirconia particles and the further modification with EDTPA to yield a support for use in separations, elsewhere. The utility r.PEZ in the separation of human immunoglobulin G (further referred to as HlgG) from cell culture supernatant and treated serum samples have been demonstrated elsewhere [2,20,26,27]. In our studies, we have used particles that were 25–38  $\mu\text{m}$  in diameter with an average pore size of  $22 \pm 4$  nm. We have attempted to understand the nature of transport of biomolecules, and identify rate limitations in mass transfer mechanisms occurring in r.PEZ. Our previous work also included the determination of adsorption profiles under various conditions. Attempts to determine the kinetic constants for the uptake of HlgG by r.PEZ and other parameters pertinent to the adsorption process have also been made [17]. Although satisfactory approximations of the kinetic constants for uptake in batch experiments were obtained; modeling of the dynamic breakthrough binding profiles at higher linear velocities and feed concentrations were less than satisfactory. In this research study, the contributions of the mass transfer mechanisms that occur during the adsorption of HlgG to r.PEZ have been investigated by pulse injection techniques.

## 2. Materials and methods

### 2.1. Reagents

All chemicals were of analytical-grade or better. Sodium chloride was purchased from Fischer Scientific (Hanover Park, IL, USA). *N,N,N',N'*-ethylenediaminetetramethylphosphonic acid (EDTPA) was purchased from TCI America (Portland, OR, USA). Bovine serum albumin (BSA), pure human immunoglobulin G was obtained from Sigma (St. Louis, MO, USA). All proteins and reagents were used without further purification. An appendix that details the equation used in the modeling studies is also included.

A Genesys<sup>TM</sup> 5 model from Spectronic Instruments UV–vis spectrophotometer (Rochester, NY, USA) was used to record the adsorption measurements. A bench top microcentrifuge (Eppendorf Centrifuge 5415C) was used to sediment the r.PEZ particles for batch experiments. The equations used to model and validate various parameters are listed in Appendix A.

### 2.2. Support matrix preparation

Colloidal zirconia was spray dried to yield zirconia particles, which were further classified, modified with EDTPA and characterized as reported elsewhere [2,20]. The particle size of the beads used in this study were 25–38  $\mu\text{m}$  in diameter and had a pore size (diameter) of  $220 \pm 4$  Å [26]. r.PEZ particles were packed into a 0.46 cm i.d.  $\times$  5.0 cm length analytical column, and supplied by ZirChrom Inc. (Anoka, MN, USA).

### 2.3. Ligand binding isotherms

Batch experiments were conducted in order to determine the maximum binding capacity of the beads and the equilibrium dissociation constants. Details of the methodology may be found elsewhere [2]. This information was used to get an idea of the extent of the dynamic capacity of the column. Thereafter, dynamic ligand binding experiments were carried out in order to determine the dynamic binding capacity and dissociation constant for the column for various linear velocities of the mobile phase. Methodology is mentioned elsewhere [15,17].

### 2.4. Chromatography

For all samples, 1 ml pulse injections were made manually to the chromatographic system. The system consisted of a Chrom Tech (Apple valley, MN, USA) Iso-2000 isocratic pump in conjunction with an online Model 783 Spectroflow spectrophotometer (Ramsey, NJ, USA). The data was recorded by an SRI (Torrance, CA, USA) PeakSimple Model 203, single channel serial port online data acquiring system. Human immunoglobulin G was monitored at 280 nm by the online spectrometer. Sodium nitrate and Blue Dextran were

monitored at an absorbance of 310 and 640 nm, respectively. The absorbance of the feed and fractions were also measured at 280 nm using the spectrophotometer (Genesys 5). All pulse experiments were performed in duplicate. All buffer solutions were filtered through Chrom Tech's Metal-Free solvent (type A-427) 10  $\mu\text{m}$  UHMWPE (Ultra High Molecular Weight Polyethylene) membrane filter during the time of use. Elution of bound HIgG and regeneration of the column was carried out using elution buffer (referred to as EB henceforth) consisting of 4 mM EDTPA, 20 mM MES and 1 M NaCl.

### 2.5. Interstitial and intraparticle porosity determination

Pulse injections of 1 ml were made with Blue Dextran at a concentration of 0.5 mg/ml to estimate the packed bed or interstitial porosity under unretained conditions (i.e. dissolved in EB). Blue Dextran was detected at 640 nm using the online spectrophotometer. To determine the intra-particle porosity, Sodium Nitrate at a concentration of 0.01 M was pulsed into the system. Sodium Nitrate was monitored at 310 nm by the online spectrophotometer. Interstitial porosity was determined from the first moments obtained under various flow rates using Blue Dextran by using Eq. (A.10), thereafter the intra-particle porosity was determined from the first moment data obtained from pulse injection of sodium nitrate.

### 2.6. Extra column contribution

In order to determine the HETP contributions from the chromatographic system itself, pulse injections of HIgG dissolved in EB (4 mM EDTPA, 20 mM MES and 1 M NaCl), were made at flow rates of 0.13, 0.25, 0.50, 1.0 and 2.0 ml/min with the column off line, by connecting the upstream and downstream tubing with a coupling unit. The first and second moments of the resultant peaks were calculated and the HETP contribution of the system estimated by equation.

### 2.7. Retained and unretained HIgG HETP

The first moments for the elution peaks obtained under unretained and retained conditions are important as they determine the residence times ( $t_r$ ). Briefly, HIgG was dissolved in loading buffer (further referred to as LB), 4 mM EDTPA, 20 mM MES; with various concentrations of salt. Salt concentrations of 0.04, 0.05, 0.075, 0.1, 0.1025, 0.15 and 1 M were used. Pulse injections were made at superficial linear velocities of 0.013, 0.025, 0.05, 0.1 and 0.2 cm/s. Sample bound were eluted using EB and the profiles recorded. The first and second moments of the eluted profiles were estimated from the fit of their Gaussian profiles. The total HETP of the eluted peak was determined by using Eq. (A.12). The HETP contribution by the column alone was obtained after eliminating extra column effects,  $H' = H_{\text{tot}} - H_{\text{ec}}$ .

A plot of  $H'$  versus linear velocity under unretained conditions permits the calculation of  $D_p$  and  $k_f$  using Eq. (A.7) and the values of  $\varepsilon_i$  and  $\varepsilon_p$  obtained from the porosity studies. In

order to do this, the equation defining unretained HETP was fit to the data by a program written in the MATLAB environment. In this method the intercept of the data plot was initially found by simple linear regression and subsequently kept constant and as the constraint in the optimization routine. Values of  $b_0$  were determined analytically using Eq. (A.11) using the first moments of the elution peaks that were recorded earlier. The value of  $D_p$  and  $k_f$  obtained from unretained HETP, was assumed not to vary with concentration and used to curve fit Eq. (A.9) for the retained peaks.

For retained peaks, the actual HETP contribution was determined as  $H_{\text{actual}} = H' - H_{\text{film}}$ , where  $H_{\text{film}}$  was determined as an average value from the Eq. (A.3).

An approach similar to the unretained data was taken for the retained data. Namely, the intercepts of the plots were kept as the constraints. After performing constrained optimization using Eq. (A.9), the values of  $r$  and  $k_{\text{des}}$  were obtained.

### 2.8. Modeling and simulation

Data were transferred from the data acquisition system and the elution profiles obtained were approximated by a Gaussian distribution using Eq. (A.12) by a code written in MATLAB. The base line corrections were made on the basis of the first reading. The program uses the function LSQCURVEFIT that has an algorithm based on the Levenberg–Marquardt method, but has a mixed quadratic and cubic line search procedure. Parameters to other equations were also obtained in a similar fashion using the appropriate equations.

## 3. Results and discussion

The ability of r\_PEZ to selectively interact with monoclonal and polyclonal antibodies has been detailed elsewhere [2]. Our previous attempts have included the elucidation of the nature of the adsorption between r\_PEZ and immunoglobulins. We have also attempted to model the separation process by using lumped parameter estimation and approximation. Based on individual rate constants, our results predicted that the adsorptive process was more favorable than the desorptive process [17]. The breakthrough profiles obtained under dynamic loading conditions were approximated by the mathematical equations describing pore diffusion. As mentioned before, assumptions about the processes were inherent in such models [17]. Break through profiles obtained at higher linear velocities were not amenable to approximation, which led us to use pulse injection techniques in conjunction with HETP analysis to estimate the mass transfer parameters.

Previous research has shown that the adsorption process on r\_PEZ is influenced by salt concentration in the mobile phase, temperature and pH, among other physical parameters. The adsorption of immunoglobulin G was not a strong function of temperature [2]. Thus, we hypothesize that HETP would vary with salt concentration or pH. We have used an approach analogous to that described by Lenhoff [13] and applied recently

by Natarajan and Cramer [18]. We have utilized the HETP equations, obtained after transforming the general transport equation in conjunction with linear mass transfer kinetics into the Laplace domain, to determine the rate limiting mass transfer mechanism in the adsorptive process. Pulse injection techniques were resorted to under linear adsorption conditions and the HETP of the system was calculated and plotted as a function of linear velocity, with salt concentration as the secondary variable. The pulse analysis theory was developed assuming a linear equilibrium isotherm [10]. Although the basic equation describing the adsorption isotherm for our system was best approximated by a second order adsorptive and first order desorptive rate equation; which at equilibrium forms the pseudo-Langmuir isotherm—suitable adjustments were made for the operating conditions to enable experimentation to be carried out under a linear adsorption region [15]. To be consistent with our assumptions, the chromatographic operations were carried out under linear binding conditions [16]. All our experiments were carried out with a feed concentration of 0.5 mg/ml and with linear velocities up to 0.2 cm/s, values within the linear regime of the dynamic isotherm (data not included).

### 3.1. Peak approximations and analysis

The elution profiles obtained under various operating conditions were approximated by the Gaussian equation, as the use of Gaussian models eliminates the errors that may effect the second moment calculation due to instrument noise [7]. A representative plot is shown in Fig. 1, where the solid lines depict the experiment profile and the dotted line depicts the Gaussian approximation obtained. As can be seen in Fig. 1,

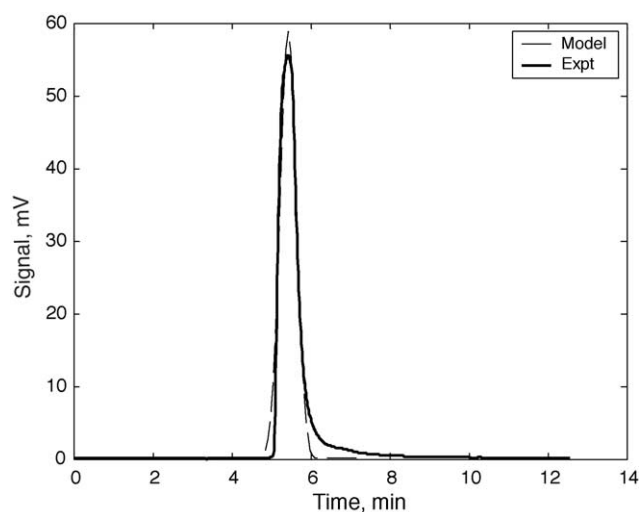


Fig. 1. Elution peaks obtained from the system were approximated with the help of the Gaussian distribution. The EMG profile was neglected for convenience. Refer to Section 1. The dashed line is the Gaussian approximation. Continuous line is the mV trace of the Ig elution peak.  $t_w$  is the peak width at half height and  $t_r$  is the retention time of the peak.

the approximations show good agreement to experimental data. Routines in MATLAB program were used to further deduce the first and the second moments for the peaks by Gaussian analysis.

### 3.2. Porosity calculation

The interstitial porosity ( $\epsilon_i$ ) of the column used estimated to be 0.39 and intraparticle porosity ( $\epsilon_p$ ) of the 25  $\mu\text{m}$  particles with a pore size of 220  $\text{\AA}$  was determined to be 0.34. These values have been used through out the calculations.

### 3.3. HETP calculations under unretained conditions

The peak profiles obtained with pulse injections of HIgG under unretained conditions were approximated by the Gaussian equation as explained earlier and the corresponding HETP was calculated using Eqs. (A.12) and (A.2). The relationship between the HETP values and the linear velocity, under unretained conditions, were carried out to estimate values of  $D_p$  and  $H_{\text{film}}$  from the corresponding  $k_f$  value. We have made an assumption that the pore diffusive flux was independent of the feed concentration. As expected, as shown in Fig. 2, under unretained conditions, separation of the molecules is minimum. It is worth mentioning that from purely a theoretical point of view, the HETP for a totally inseparable species should ideally equal infinity as theoretically there would be no stage available for separation, i.e.  $N=0$ .

A linear relationship was observed between HETP and linear velocity as shown in Fig. 2. The film mass transfer coefficient,  $k_f$ , was determined to have a value of 0.999 cm/s. The value of  $D_p$  was found to be 2.06E-8 cm<sup>2</sup>/s. The average

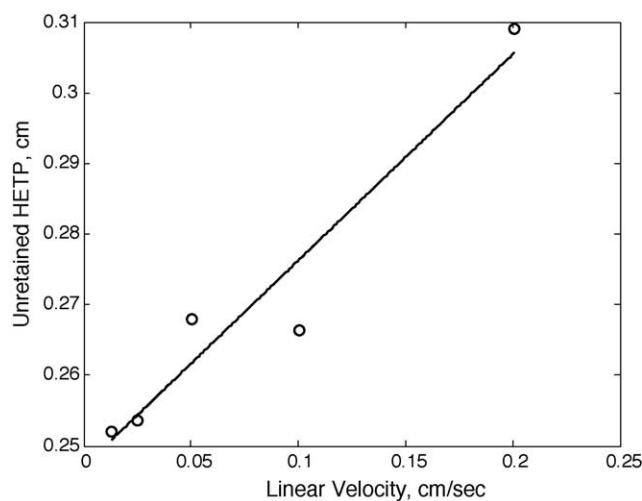


Fig. 2. HETP of the packed r.PEZ analytical column for HIgG under unretained conditions as a function of linear velocity. The values of  $k_f$  and  $D_p$  determined in this optimization were used for curve fitting the HETP profiles under retained conditions. The mobile phase consisted of 4 mM EDTPA, 20 mM MES and 1 M NaCl at pH 7.0.



$H_{\text{film}}$  for the system was calculated as  $4.02\text{E-}5$  cm. The values obtained in this step were used to for subsequent calculations. A tortuosity factor of 0.875 was determined for the zirconia particles used in this study.

### 3.4. HETP calculations under retained conditions

The peak profiles obtained with pulse injections of HIgG under retained conditions were approximated by the Gaussian equation as explained earlier and the corresponding HETP was calculated using Eqs. (A.12) and (A.2). It was assumed that the variance in the HETP contribution due to film mass transfer was negligible under the range of the linear velocities of operation. An  $H_{\text{film}}$  value of  $4.02 \times 10^{-5}$  cm obtained from unretained HETP data was subtracted from the retained HETP data, in order to negate its influence on the actual HETP of the column. Fig. 3 shows the variance of HETP with respect to superficial linear velocity and salt concentration. HETP is seen to increase with increasing velocity for any given salt concentration. HETP is also seen to increase with increase in salt concentration in the feed buffer (LB) for the same superficial linear velocity.

### 3.5. Determination of $r$ and $k_{\text{des}}$

Linear regression analysis was used to curve fit the data depicted in Fig. 3 and the values of the slope and intercept were further determined. For each value of the slope and its corresponding  $b_0$  value was determined using Eq. (A.11) from the first moment of the elution profile. The parameters were determined employing Eq. (A.9) under the constraint

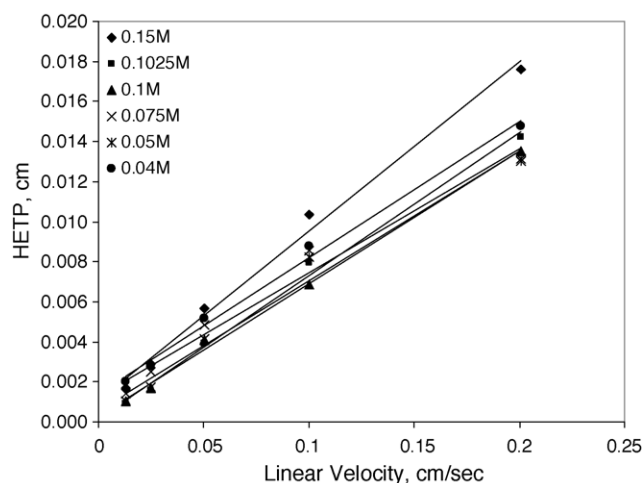


Fig. 3. Variation of HETP with linear velocity for different salt concentrations. Data profile determined by least squares fit. HIgG was fed into the analytical column (0.46 cm i.d.  $\times$  5 cm  $L$ ) packed with r-PEZ. Salt concentrations used are as indicated and operations using the same were carried out by changing the respective loading buffers' salt composition. The elution and regeneration buffers' salt composition remained the same, i.e. 1 M NaCl. The equilibrating and diluting buffer was the same as the loading buffer.

that  $r$  is non-negative. The values obtained for  $r$  and  $k_{\text{des}}$  are  $1.06 \text{E-}4$  and  $1.44 \text{E}03$ , respectively.

The axial dispersion,  $D_a$ , of the chromatographic system was observed to vary with salt concentration.  $D_a$  values were calculated from the intercept values obtained from the linear regression model of HETP versus linear flow rate. It can be logically argued that for a given flow rate and feed concentration, the amount of adsorbate in the system is dependent on the physical parameters influencing the adsorption process. In our case it was salt concentration of the buffer. The concentration of adsorbate in the system increases for the same feed concentration and linear velocity with increasing salt concentration, as higher salt concentration inhibits the adsorption process. At low salt concentration, the protein molecules will have a tendency to disperse minimally in the axial direction and more along the length of the column due to convective effects. The axial dispersion increases though, with increasing salt concentration as now more protein molecules are present in the system and have to occupy the same space available with the moving front. Thus it is incorrect to assume that for a given system the axial diffusion remains constant and is independent of the adsorbate concentration in the column under the same feed concentration, let alone linear velocity. This assumption may be valid at the entrance though, but not inside the column matrix. Similar arguments hold for ion-exchange systems.

The profile also indicates that the variation in axial dispersion may be neglected under retained conditions, as indicated by the intercepts that lie in close proximity (Fig. 3).

The correlation proposed by Foo and Rice [25],

$$Sh = 2 + 1.45(Re)^{1/2}(Sc)^{1/3}$$

has usually been used to estimate the value of the film mass transfer coefficient,  $k_f$ . However, during the optimization process it was found that the values of  $k_f$  as determined by the correlation did not fit the data properly. As stated by Arnold et al. [10], this correlation only gives an estimation of the appropriate  $k_f$  value. The  $k_f$  values were thus determined independent of this correlation while fitting the data. An idea of the range of the  $k_f$  values were obtained using this correlation and values determined after applying the least squares curve fit method to our data set was compared to it. It is unclear whether previous studies [18] have assumed that the film mass transfer coefficient to be constant or not. It is evident from the correlation though that  $k_f$  is dependent on the linear velocity.

The  $k_f$  values using constrained optimization routine for the retained HETP data were determined after suitable substitution with the  $b_0$  values obtained as mentioned earlier. Hence, ranges of values were obtained, and the corresponding  $H_{\text{film}}$  for each salt concentration and linear velocity was subtracted to obtain the actual HETP contribution. A linear regression of this data then gave the actual slope values that were used to determine the parameters in Eq. (A.9).

Table 1  
The theoretical number of transfer units—definitions

NTU <sup>a</sup>	Description
$N_p = \frac{D_p L}{R^2 u}$	Pore diffusion: convective transfer
$N_s = \left( \frac{1-\varepsilon_p}{\varepsilon_p} \right) \frac{D_s L}{R^2 u} \left( \frac{q}{c} \right)$	Surface diffusion: convective transfer
$N_f = \frac{3k_f L}{Ru}$	Film mass transfer: convective transfer
$N_{des} = \frac{k_{des} L}{u}$	Desorption kinetics: convective transfer

<sup>a</sup> The NTU defined in this article is equivalent to the dimensionless numbers reported by Natarajan and Cramer [14].

The curve fitting of the data using Eq. (A.9) is dependent on the value of  $r$ . It was observed that for values of  $r$ , the ratio of surface to pore diffusion, not equal to zero the profile reached a distinct maximum. This is in agreement to the observation reported by Natarajan and Cramer [18]. Results indicate that the pore diffusion is the rate determining step in the mass transfer mechanisms controlling the adsorptive process, as surface diffusion can be considered to be absent ( $r=1.06E-4$ ). Table 1 lists the definitions of various parameters that impact the mass transport of HIgG in r-PEZ. These are nothing but the theoretical number of transfer units (NTU) contributed by various mass transfer mechanisms in the chromatographic system. The NTU contribution due to axial dispersion was not reported, as it was argued before that it is a function of the solute concentration also. The exact relationship of the same is currently unknown. Table 2 shows the relationship of the various NTUs. They are all functions of velocity and for any given superficial linear flow rate can be easily estimated and their values compared to determine the rate limiting mechanism. The  $N_s$  and  $N_{des}$  incorporate terms that are influenced by the salt concentration of the system. It is seen that  $N_{des}$  and  $N_f$  values differs from the  $N_p$  value by at least two orders of magnitude. This implies that the rate limiting mechanism is pore diffusion. This is a reasonable conclusion given the fact that the size of an IgG molecule is around 10 nm (effective diameter of 8.5–10.0 nm). By inserting different values for the ratio of the solute or biomolecule ( $R_s$ ) to the pore radius ( $R_p$ ) in the Renkin's equation, one finds that the pore diameter should be at least five times the diameter of the solute to avoid severely restricted rates of diffusion. Thus for applications involving IgG transport and binding, the support pore diameter should be in the range of 43–50 nm. The pore diameter of the zirconia support used in this study was 22 nm thus making our conclusions quite relevant. In a previous study [17] this was assumed for the modeling of the dynamic break

Table 2  
NTU contribution for HIgG using r-PEZ

Matrix	$N_p$	$N_s$	$N_{des}$	$N_f$
r-PEZ	0.026/ $u$	No surface diffusion	9670/ $u$	8693/ $u$

Various NTUs determined as per definition in Table 1.

through profiles and this result validates our assumption. Hence, to accurately model the system, numerical methods of solving the relevant transport equations should be resorted to.

## 4. Conclusion

Our results have highlighted the need to further optimize the surface area, pore size, and pore volume for the retention and separation of biologically relevant biomolecules as we have found that, the transport of biomolecules in the zirconia particles with a pore size of 22 nm [26] is limited by pore diffusion. Based on our current work, that have enabled the preparation of porous zirconia particles by *spray-drying* of colloidal zirconia suspension, the logical next step is to further optimize the spray-drying or the PICA process to produce particles with varying sizes and controlled pore architecture. The *current and future directives* of our research are to develop methods to produce zirconia particles and monoliths of varying particle sizes with controlled and hierarchical pore structure, and to further modify zirconia surfaces with polymers, inorganic, or organic substrates to yield chemically bonded zirconia surfaces with novel selectivities.

## 5. Nomenclature

$b_0$	mass partition coefficient
$D_a$	axial dispersion co-efficient (cm <sup>2</sup> /s)
$D_p$	pore diffusion co-efficient (cm <sup>2</sup> /s)
$D_s$	surface diffusion coefficient (cm <sup>2</sup> /s)
$F$	flow rate (ml/min)
$H_{tot}$	total height equivalent to a theoretical plate (HETP) of the system (cm)
$H_{ec}$	extra column contribution to the HETP (cm)
$H'$	HETP of the column (cm)
$H_{film}$	HETP contribution from film mass transfer (cm)
$k_{des}$	desorption rate constant
$k_f$	film transport coefficient (cm/s)
$L$	length of column (cm)
$r$	ratio of surface to pore diffusion
$R$	particle radius (m)
$S$	slope of HETP versus $u$ plots (s)
$t_{w,1/2}$	width at half height (min)
$t_r$	retention time (min)
$u$	superficial velocity (cm/s)
$V_0$	column dead volume (ml)

### Greek characters

$\varepsilon_i$	interstitial porosity
$\varepsilon_p$	particle porosity
$\mu_1$	first moment
$\sigma_{ec}$	square of variance (min)

## Appendix A

The HETP contribution by the column alone ( $H'$ ) was obtained after eliminating extra column effects,

$$H' = H_{\text{tot}} - H_{\text{ec}} \quad (\text{A.1})$$

For retained peaks, the actual HETP contribution was determined as

$$H_{\text{actual}} = H' - H_{\text{film}} \quad (\text{A.2})$$

where  $H_{\text{film}}$  was determined as (where  $k_f$  values were determined analytically from experimental data of the unretained elution profiles).

$$H_{\text{film}} = \frac{2(1 - \varepsilon_i)\varepsilon_p u}{\{\varepsilon_i + (1 - \varepsilon_i)\varepsilon_p\}} \left( \frac{R}{3k_f} \right) \quad (\text{A.3})$$

In this paper the reaction-dispersive model was investigated. The following equation relates the effect of salt concentration and linear velocity to the total HETP (without extra column HETP contribution) [18]:

$$H = \frac{2D_a}{uL} + \frac{2(1 - \varepsilon_i)\varepsilon_p b_0^2 u}{\{\varepsilon_i + (1 - \varepsilon_i)\varepsilon_p b_0\}^2} \times \left[ \frac{R}{3k_f} + \frac{R^2}{15D_p(1 + \{b_0 - 1\}r)} + \frac{(b_0 - 1)}{b_0^2 k_{\text{des}}} \right] \quad (\text{A.4})$$

where  $\varepsilon_i$  is the intra-particle porosity,  $R$  the radius of the matrix particle,  $D_p$  the pore diffusivity,  $k_{\text{des}}$  is the desorption rate constant and  $r$  and  $b_0$  are defined as

$$r = \frac{D_p}{D_s} \quad (\text{A.5})$$

$D_s$  is the surface diffusion coefficient.

$$b_0 = 1 + k' \quad (\text{A.6})$$

and  $k'$  is the mass distribution ratio. Determination of  $k'$  values for the system have been discussed in the later part of this section.

Under unretained conditions,  $b_0$  is equal to 1 as no adsorption of solute to the matrix occurs (i.e.  $k' = 0$ ) and Eq. (A.1) simplifies to [18]:

$$H = \frac{2D_a}{uL} + \frac{2(1 - \varepsilon_i)\varepsilon_p u}{\{\varepsilon_i + (1 - \varepsilon_i)\varepsilon_p\}^2} \left[ \frac{R}{3k_f} + \frac{R^2}{15D_p} \right] \quad (\text{A.7})$$

For retained conditions, subtracting the HETP contributed by film mass transfer, Eq. (A.3) becomes [18]:

$$H = \frac{2D_a}{uL} + \frac{2(1 - \varepsilon_i)\varepsilon_p b_0^2 u}{\{\varepsilon_i + (1 - \varepsilon_i)\varepsilon_p b_0\}^2} \times \left[ \frac{R^2}{15D_p(1 + \{b_0 - 1\}r)} + \frac{(b_0 - 1)}{b_0^2 k_{\text{des}}} \right] \quad (\text{A.8})$$

The slope of Eq. (A.8) is a function of  $b_0$ , which maybe written after differentiating it with respect to  $u$  as,

$$S = \frac{2(1 - \varepsilon_i)\varepsilon_p b_0^2}{\{\varepsilon_i + (1 - \varepsilon_i)\varepsilon_p b_0\}^2} \times \left[ \frac{R^2}{15D_p(1 + \{b_0 - 1\}r)} + \frac{(b_0 - 1)}{b_0^2 k_{\text{des}}} \right] \quad (\text{A.9})$$

### A.1. Porosity determination

The porosity of the column is related to the first moment and linear velocity as

$$\mu_1 = \frac{L}{u} (\varepsilon_i + (1 - \varepsilon_i)\varepsilon_p b_0) \quad (\text{A.10})$$

Rearrangement of Eq. (A.10) allows the calculation of  $b_0$  as follows:

$$b_0 = \frac{1}{(1 - \varepsilon_i)\varepsilon_p} \left[ \mu_1 \frac{u}{L} - \varepsilon_i \right] \quad (\text{A.11})$$

where  $L$  the length of the column,  $u$  is the linear velocity,  $\varepsilon_i$  is the interstitial porosity and  $\varepsilon_p$  is the intra-particle porosity and  $b_0$  is the parameter reflecting retention factor. Under unretained conditions  $b_0$  is equal to 1 by definition.

### A.2. HETP determination

The elution profiles obtained were approximated with a Gaussian profile and the first and second moments were determined. The total HETP of the Gaussian profile was determined using the following equation

$$H_{\text{tot}} = \frac{L}{5.54} \left( \frac{t_{w,1/2}}{t_r} \right)^2 \quad (\text{A.12})$$

Where  $t_{w,1/2}$  is the width of the Gaussian profile at half height and  $t_r$  is the retention time.

The extra column contribution was determined by the following equation:

$$H_{\text{ec}} = L \left( \frac{\sigma_{\text{ec}} F}{V_0 b_0} \right)^2 \quad (\text{A.13})$$

where  $\sigma_{\text{ec}}$  is the second moment of the resultant peak,  $V_0$  is the column dead volume,  $b_0$  is the mass partition coefficient (in this case equal to one as all species are non binding) and  $F$  is the flow rate.

## References

- [1] J. Bonnerjea, S. Oh, M. Hoare, P. Dunnhill, *Biotechnology* 4 (1986) 954.
- [2] A. Subramanian, S. Sarkar, *J. Chromatogr. A* 944 (2002) 179.
- [3] N.B. Afeyan, S.P. Fulton, F.E. Regnier, *J. Chromatogr.* 544 (1991) 267.

- [4] P. Miroslav, S. Frantisek, J.M.J. Frechet, *J. Chromatogr. A* 752 (1996) 59.
- [5] M. Leonard, *J. Chromatogr. A* 699 (1997) 3.
- [6] M.A. Fernandez, G. Carta, *J. Chromatogr. A* 746 (1996) 169.
- [7] G. Guiochon, S. Golshan Shirazi, A.M. Katti, *Fundamentals of Preparative and Non-linear Chromatography*, Academic Press, New York, NY, 1994.
- [8] A. Liapis, *Sep. Purif. Methods* 19 (1990) 133.
- [9] F.H. Arnold, J.J. Chalmers, M.S. Saunders, M.S. Croughan, H.W. Blanch, C.R. Wilke, *Purif. Ferm. Prod.* (1985) 114.
- [10] F.H. Arnold, H.W. Blanch, C.R. Wilke, *Chem. Eng. J.* 30 (1985) B25.
- [11] F.H. Arnold, H.W. Blanch, *J. Chromatogr.* 355 (1986) 13.
- [12] F.H. Arnold, H.W. Blanch, C.R. Wilke, *Chem. Eng. J.* 30 (1985) B9.
- [13] A.M. Lenhoff, *J. Chromatogr.* 384 (1987) 285.
- [14] H.A. Chase, *J. Chromatogr.* 297 (1984) 179.
- [15] H.A. Chase, *Chem. Eng. Sci.* 39 (1984) 1099.
- [16] S. Sarkar, A. Subramanian, *J. Chromatogr. A* 790 (2003) 143.
- [17] S. Sarkar, Masters thesis, University of Minnesota, Saint Paul, MN, 2002.
- [18] V. Natarajan, S. Cramer, *Sep. Sci. Tech.* 35 (2000) 1719.
- [19] J. Nawrocki, M.P. Rigney, A. McCormick, P.W. Carr, *J. Chromatogr. A* 657 (1993) 229.
- [20] A. Subramanian, P.W. Carr, C.V. McNeff, *J. Chromatogr. A* 890 (2000) 15.
- [21] J.B. Rosen, *J. Chem. Phys.* 20 (1952) 387.
- [22] M. Kubin, *Collect. Czech. Chem. Commun.* 30 (1965) 2900.
- [23] E. Kucera, *J. Chromatogr.* 19 (1965) 237.
- [24] Cs. Horvath, H-J. Lin, *J. Chromatogr.* 149 (1978) 43.
- [25] S.C. Foo, R.G. Rice, *AIChE J.* 45 (1975) 1149.
- [26] A. Subramanian, P.W. Carr, C.V. McNeff, S. Sarkar, *J. Chromatogr. A* 790 (2003) 143.
- [27] M.C. Mowry, M.M. Meagher, L. Smith, J. Marks, A. Subramanian, *Protein Exp. Purif.* 37 (2004) 399.